



Bulletin of the Mineral Research and Exploration

<http://bulletin.mta.gov.tr>



Interpretation of satellite gravity anomalies with pseudo-depth slicing method filter in Türkiye

İlkin ÖZSÖZ^{a*} and Ceyhan Ertan TOKER^a

^aGeneral Directorate of Mineral Research and Exploration, Ankara, Türkiye

Research Article

Keywords:

Satellite Gravity Data, Spectral Methods, Pseudo-Depth Slicing Method, Radial Average Power Spectrum, Qualitative Interpretation.

ABSTRACT

In this study, discontinuities and major tectonic boundaries are interpreted in and around Türkiye by Bouguer gravity anomaly. The World Gravity Map 2012 is used for the interpretation of major tectonic features in the Anatolia Region. Radial average power spectrum (RAPS) and band-pass filter are used for long and short wavelength separation. For the whole study area, four depth segments are detected. Moreover, the radial average depths of these depth segments are 54.9 km, 32.2 km, 21.9 km and 8.0 km. In order to conduct better interpretation, the study area was divided into three subareas from the west to the east (area 1 to area 3). In area 1 (41.4 km, 21.2 km and 7.8 km) and area 2 (48.1 km, 20.0 km and 6.6 km), three depth sources are detected. Furthermore, four various depth segments are analysed in area 3 (54.3 km, 29.8 km, 20.8 km and 8.6 km). The interpretation of the whole study area, area 1, area 2 and area 3 showed that depth of the sediment accumulation in the Western Anatolia is estimated as 7.8 km.

Received Date: 26.03.2021

Accepted Date: 26.07.2021

1. Introduction

The gravity anomalies can be considered as the sum of the long and short-wavelength components. In general, the short-wavelength components can be associated with the near-surface geological structures while the long-wavelength components likely to indicate the deep-seated structures. The anomalous body can be estimated from short or long-wavelength components concerning its depth and size (Arfaoui et al., 2011).

The short and long wavelength components can be identified by interpreting the regional or residual part of the observed data. There are various methods for regional-residual separation, which can be applied via least-squares fitting of polynomial surfaces

(Simpson, 1954), spectral factorization (Gupta and Ramani, 1980), frequency domain operations, Wiener filters (Pawłowski and Hansen, 1990), finite element method (Mallick and Sharma, 1999) and matrix smoothing method by average weighting process (Arfaoui et al., 2011).

In this study, the gravity anomaly, obtained from World Gravity Map 2012 (WGM 2012) (Bonvalot et al., 2012) is analysed. WGM 2012 includes land, marine, airborne and satellite gravity data as well as satellite altimetry data. Geophysical and geodetic characteristics of gravity anomaly are taken into account during computing WGM 2012 (Bonvalot et al., 2012). Bouguer and terrain correction is computed by 1°*1' resolution topography and bathymetry ETOPO1 (Amante and Eakins, 2009) grid. Additionally, the

Citation Info: Özsoz, İ., Toker, C. E. 2022. Interpretation of satellite gravity anomalies with pseudo-depth slicing method filter in Türkiye. Bulletin of the Mineral Research and Exploration 168, 111-130. <https://doi.org/10.19111/bulletinofmre.974936>

*Corresponding author: İlkin ÖZSÖZ, ilkin.ozsoz@mta.gov.tr

atmospheric mass effect is removed from the observed data (Bonvalot et al., 2012).

There were many previous studies (Ateş et al., 1999, 2012; Arslan, 2016) about gravity and magnetic interpretation in Türkiye. Western Anatolia is investigated by Sari et al. (2002), Tirel et al. (2004), Doğru et al. (2017) and Kahveci et al. (2019). Additionally, Büyüksaraç et al. (2005), Onal et al. (2008), Oruç (2011), Bilim (2017a) and Bilim et al. (2017b) interpreted the Central Anatolia region via gravity and magnetic data. Finally, tectonic and crustal structures in the Eastern Anatolia are evaluated by Pamukçu et al. (2007), Büyüksaraç (2007), Maden et al. (2009) and Pamukçu et al. (2015).

The aim of this paper is to decompose superimposed geological structures in terms of their wavenumber component and interpret the regional tectonic boundaries and discontinuities between 22° E and 45° E, 35° N and 42°N. In order to improve the interpretation phase, the study area is divided into three particular subareas (area 1, area 2, and area 3). The whole study area and the sub-areas are interpreted by the spectral analysis method which was proposed by Spector and Grant (1970). The average depth of causative bodies is estimated by this method.

Throughout this paper, variations of the tectonic structures with depth and wavenumber will be interpreted. The combination of the RAPS and band-pass filter provides characteristics of the tectonic elements for the certain wavenumber interval. Although a variety of papers were previously published, interpreting the geological structures of Türkiye, none of which had taken into account the variations of these structures with respect to depth. This paper was undertaken to explain the spatial distribution of the tectonic elements within the different wavenumber intervals via the pseudo-depth slicing method, which was proposed by Arfaoui et al. (2011).

2. Tectonic Settings

The study area is located in the seismically active zone and it comprises various tectonic regimes. Figure 1 illustrates the boundaries of the study area. Although the study area comprises many different countries, Türkiye is the major target of this paper. The tectonic activity in the study area initiated with the continental

collision of the Eurasian and African plates (Şengör and Kidd, 1979; Şengör and Yılmaz, 1981; Okay and Tüysüz, 1999; Bozkurt and Mittweide, 2001; Moix et al., 2008; Göncüoğlu, 2010).

Historically, the location of the study area corresponds to the boundary between two megacontinents, Laurasia and Gondwana (Durand et al., 1999; Bozkurt and Mittweide, 2001). These megacontinents provided distinctive lithospheric fragments which amalgamated when the Arabian plate collided with the Anatolian plate (Bozkurt and Mittweide, 2001). The development of the Tethyan oceans might be related to the spatial characteristics of the megacontinents (Bozkurt and Mittweide, 2001; Robertson, 2004; Robertson et al., 2009).

The existence of two Tethyan oceans, Paleotethys and Neotethys, can be tracked back by age and distribution characteristics of subduction complexes and ophiolites (Şengör, 1979, 1987; Şengör and Yılmaz, 1981; Okay and Tüysüz, 1999; Stampfli, 2000; Bozkurt and Mittweide, 2001). The southern Neotethys, Intra-Pontide, and the northern Neotethys are the oceanic basins that are related to the Neotethys (Bozkurt and Mittweide, 2001). The latter two no longer exist but the southern Neotethys can be observed in the Eastern Mediterranean Sea (Robertson and Shallo, 2000).

It is worth noting that there are different models that explain evolution of Tetyhs oceans in Türkiye (Şengör and Yılmaz, 1981; Okay and Tüysüz, 1999; Ustaömer and Robertson, 1999; Göncüoğlu et al., 2000; Stampfli, 2000; Elmas and Yiğitbaş, 2001).

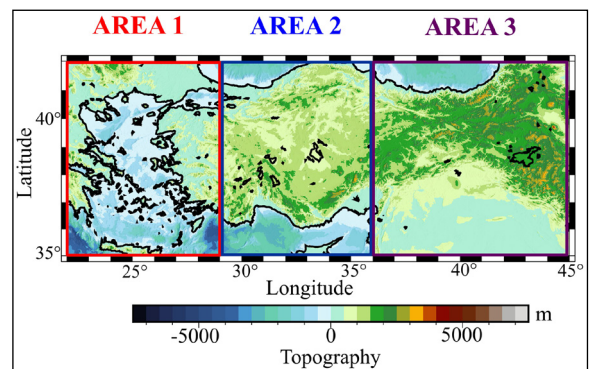


Figure 1- Location map of the study area and subareas (areas 1, 2 and 3).

Okay and Tüysüz (1999) suggested that Türkiye can be divided into five major suture zones which are Intra-Pontide, Southeast Anatolian, Inner Tauride, Antalya, and İzmir-Ankara-Erzincan. According to Ketin (1966), Pontides, Anatolides, Taurides, and bounding faults are subdivisions of Anatolia.

Pontides (Triassic age) located in the northern part of the study (Bozkurt and Mittwede, 2001). The tectonic patchwork of Pontides includes three major zones (Okay, 1989) which are Strandja Zone (Okay et al., 2001), İstanbul Zone (Aydın et al., 1986; Görür et al., 1997; Dean et al., 2000) and Sakarya Zone (Bingöl et al., 1975; Şengör et al., 1980; Şengör and Yılmaz, 1981; Tekeli, 1981; Koçyiğit, 1987, 1991; Altiner et al., 1991; Altiner and Koçyiğit, 1993; Genç and Yılmaz, 1995; Okay and Monie, 1997; Rojay and Altiner, 1998; Kozur et al., 2000).

In the southern part, Anatolides and Taurides are treated together (Tauride-Anatolide platform) by Şengör and Yılmaz (1981). Bornova flysch zone (Erdoğan, 1990), Tavşanlı zone (Harris et al., 1994; Sherlock et al., 1999), Afyon zone (Özcan et al., 1988), Menderes Massif and Central Anatolian Crystalline Complex are comprised by Anatolide platform. Furthermore, the Tauride platform includes unmetamorphosed nappes, comprised of carbonates, turbidites, and clastic rocks (Özgül, 1976, 1985).

The southeastern part of the study area is characterized by the juxtaposition of Arab and Tauride-Anatolide platforms (Ketin, 1966; Yılmaz, 1993; Yılmaz and Yıldırım, 1996). Additionally, the Arabian platform might have a major contribution to potential hydrocarbon production in Türkiye.

Paleozoic sedimentary rocks and nappe structures are observed in the Anatolide-Tauride block (Bozkurt and Mittwede, 2001). Unlike Taurides, ubiquitous regional metamorphism is noted in the Anatolide block (Okay et al., 2001). Nappe structures are common in the Taurides whereas deformed, sliced and metamorphosed rocks are characteristics of the Anatolide block (Bozkurt and Mittwede, 2001).

In the Late Miocene-Pliocene, intra-continental convergence was initiated between the Tauride-Anatolide platform and Pontides (Bozkurt and Mittwede, 2001). Consequently, N-S shortening was

initiated in the study area. At the present time, N-S compression continues in the only eastern part of Türkiye (Dewey et al., 1986; Şaroğlu and Yılmaz, 1986; Bozkurt and Mittwede, 2001; Faccenna et al., 2006; Keskin, 2007; Göğüş and Psyklywec, 2008).

The Miocene sedimentation is ubiquitous in the study area. In western Anatolia, there are many E-W trending grabens. Furthermore, foreland basins are noted in the Tauride platform (Legeay et al., 2016). In Pontides and Anatolides, Miocene sedimentation developed as collision-related basins (Görür et al., 1998; Kaymakçı et al., 2000; Ocakoğlu et al., 2001; Catto et al., 2018; Gülyüz et al., 2019). In addition, Görür et al., (2000) indicated that marine carbonates and clastic sediments in the Pontides are associated with the Paratethys.

In the eastern part of the study area between Eurasia and the Arabian platform, Miocene sedimentation is characterized by reefal limestones, turbidites, and marine carbonates (Bozkurt and Mittwede, 2001). The closure of the Bitlis Ocean was initiated by the convergence between the Arabian and Anatolian Plate in the Late Miocene (Bozkurt and Mittwede, 2001). This intracontinental convergence results in uplift and crustal thickening in the eastern part of the study area. Consequently, the Southeast Anatolian Suture occurred. The tectonic regime of Eastern Anatolia converted from a compressional-contractual regime to a new compressional regime in the neotectonic period (Bozkurt and Mittwede, 2001).

Türkiye can be divided into three major structures in terms of neotectonic framework: North Anatolian Fault Zone (Ketin, 1969), East Anatolian Fault Zone, and Aegean Cyprian Arc (Figure 2). Firstly, the dextral North Anatolian Fault Zone and the sinistral East Anatolian Fault Zone are intracontinental transform faults. Secondly, Aegean Cyprian Arc is the convergent plate boundary. Another fault that has an impact on the neotectonics of Türkiye is the sinistral Dead Sea Fault. In northeast Türkiye, a continental triple junction formed where two strike-slip faults coincided (Karig and Kozlu, 1990).

Rotstein (1984) suggested that the amalgamated crustal fragment is moving to the west. Hence, the westward extrusion results in a counter-clockwise

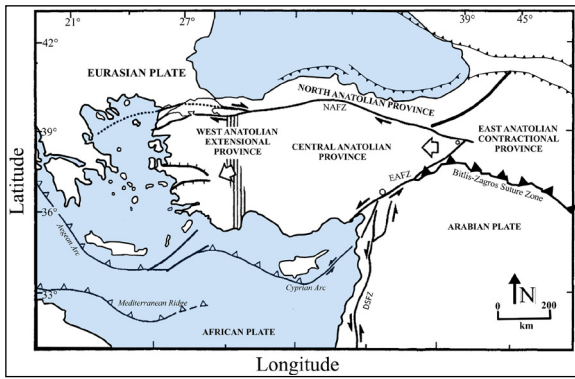


Figure 2- Simplified tectonic map of the study area (modified from Şengör et. al., 1985; Bozkurt and Mittwede, 2001). NAFZ= North Anatolian Fault Zone, EAFZ= East Anatolian Fault Zone, DSFZ= Dead Sea Fault Zone).

rotation of Anatolia. The internal deformation of Anatolia stems from the NAFZ, EAFZ and the westward movement of Anatolia (Bozkurt and Mittwede, 2001). Şengör et al. (1985) divided Anatolia into four Neotectonic provinces; the East Anatolian contractual, West Anatolian extensional, the Central

Anatolian and the North Anatolian provinces. Major structures and continental blocks of the study area is illustrated in Figure 3.

3. Method

3.1. Radially Averaged Power Spectrum (RAPS)

Bhattacharyya (1966) mentioned the fundamentals of spectral analysis in terms of magnetic sources. The power spectrum is generally based on the geometry of sources instead of the source parameter (Maus and Dimri, 1995).

Spector and Grant (1970) introduced the RAPS. Radial (or Azimuthal) variation of the power spectrum can be expressed as

$$S^2(k) = [e^{(-4\pi k)}][1 - e^{(-4\pi k)^2}(A^2(k\phi))] \quad (1)$$

where $S^2(k)$ is the radial power spectrum and k is the wavenumber. The term $[e^{(-4\pi k)}]$ represents radial

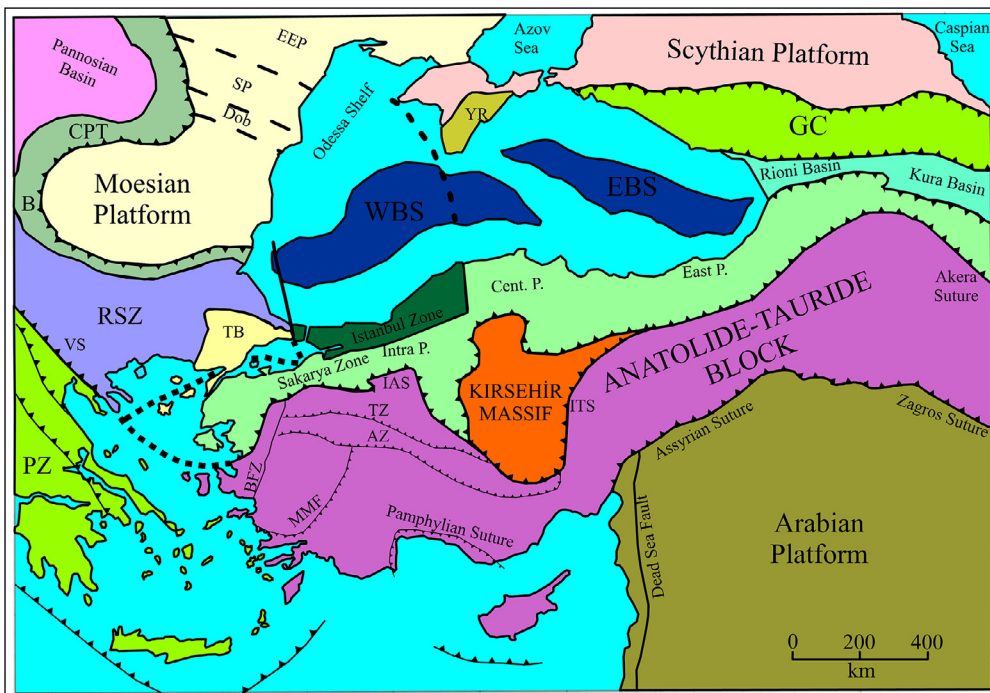


Figure 3- Continental blocks and major structures of northeast Mediterranean (modified from Şengör, 1984; Okay, 1989; Okay et. al., 1994; Okay and Tüysüz, 1999). PZ= Pelagonian Zone, VS= Vardar Suture, RSZ= Rhodope-Strandja Zone, B= Balkanides, CPT= Carpathians, Dob= Dobrudja, SP= Scythian Platform, EEP= East European Platform, YR= Yayla Range, WBS=West Black Sea Basin, EBS= East Black Sea Basin, GC= Greater Caucasus, Intra P.= Intra Pontide Suture, Cent. P.= Central Pontides, East P.= Eastern Pontides, IAS= İzmir - Ankara Suture, TZ= Tavşanlı Zone, AZ= Afyon Zone, MMF= Menderes Massif, BFZ= Bornove Flysch Zone).

averaging. $A^2(k\phi)$ denote the dimensions of prisms along the horizontal plane. Hence Equation 1 can be written as

$$S^2(k) = f(\phi) * f(t) * f(\phi) \tag{2}$$

where $f(h)$ is depth, $f(t)$ is depth extent, and $f(\phi)$ is the size factor. The major contribution comes from depth (Fairhead, 2016).

The prominent advantage of this method is depth estimation can be applied to the observed data (Fairhead, 2016). Regional and residual separation is not required. Furthermore, Spector and Grant (1970) mentioned that each linear segment represents an average depth. On the other hand, the apparent drawback of the RAPS is powers, which are averaged, is not fitting the same wavenumber (Maus and Dimri, 1995).

RAPS may detect more than one source. In this case, the anomaly can be separated by using appropriate filters.

3.2. Filter Design

Saramaeki et al. (1993) mentioned the fundamentals of filter design. Filter design is an iterative process. If the designed filter does not provide the desired response, filter properties (cut-off frequency, filter degree, etc.) should be adjusted. Error in the observed data is the other contributor that affects the response of the filter.

The primary drawback of the steep filters is the Gibbs phenomenon. The Gibbs phenomenon results in side-lobes which may seriously affect the interpretation of the data (Gottlieb and Shu, 1997).

Therefore, fixed window functions are used for reducing the effect of the Gibbs phenomenon. The window function tapers the designed filter smoothly. In this study, the Gaussian window is used for tapering the filter. Figure 4 shows the schematic illustration of the designed filter and its windowed version by Gaussian window.

3.3. Pseudo Depth Slicing

Depth estimation and source estimation can be estimated from the log-log plot of the squared amplitude spectrum. Fairhead (2016) suggested that it can be a powerful tool in terms of regional-residual separation.

The gravity anomaly grid can be considered as the sum of anomalies from various depth segments. The anomaly grid can be represented via RAPS (Spector and Grant, 1970).

Generally, the long-wavelength anomalies in the RAPS are associated with the deeper regional structures. However, Fairhead (2016) emphasizes that shallow structures may have long-wavelength components. This phenomenon should be taken into account during regional-residual separation.

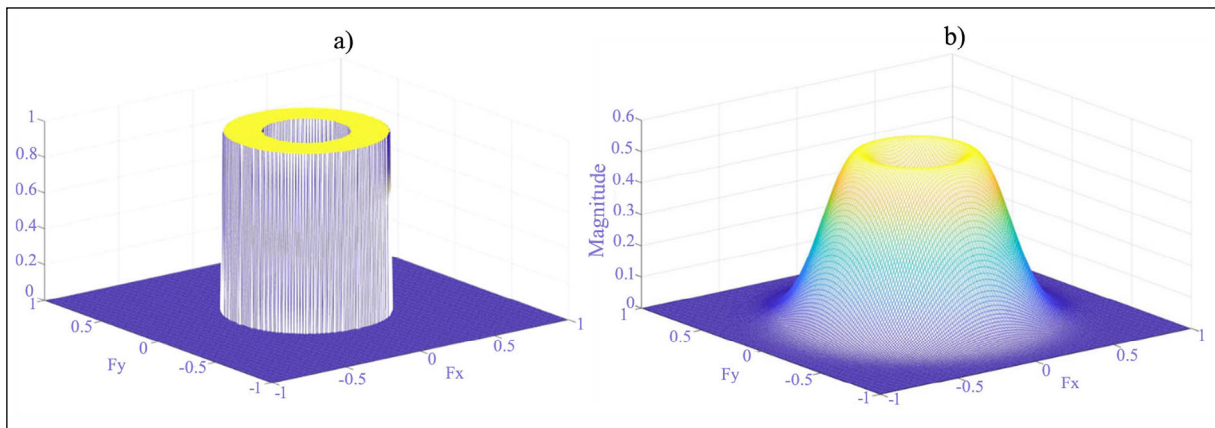


Figure 4- Schematic demonstration of desired and applied filters; a) the desired filter that is susceptible to the Gibbs phenomenon, b) applied filter, windowed by Gaussian window. It has more gentle slopes.

Desired wavelength components can be filtered with the help of the power spectrum. If only the long-wavelength components of the power spectrum are targeted, the swing-tail filter can be used. According to Cordell and Grauch (1985), the swing-tail filter suppresses a high-frequency tail that follows the linear segment. In general, near-surface anomalies and noise are removed from data. Fairhead (2016) recommended that after the swing-tail filter, Euler deconvolution or the other automated depth estimation technique can be used.

On the other hand, the swing-head filter is exactly the opposite of the swing-tail filter. It suppresses long-wavelength components. Consequently, shorter wavelength components can be interpreted clearly. It should be noted that if there is one linear segment on the RAPS, this filter cannot be applied.

Swing-tail and swing-head filters provide deep and shallow sources respectively. However, if the desired depth is an intermediate depth, a band-pass filter ought to be used. The result will contain short and long-wavelength components of data. Moreover, two depth slices were filtered. For obtaining the depth slice of intermediate depths, at least three linear segments are required on the power spectrum.

Figure 5 briefly explains the pseudo-depth slicing method. For instance, depth slices with shorter wavelength (or higher wavenumber) components can be obtained by swing head filter.

The obvious advantage of the pseudo depth slicing method is separating anomalies from various depths. Moreover, it isolates anomalies between desired wavelengths.

3.4. Edge Detection Process

Geosoft Oasis Montaj's Centre for exploration (CET) extension was used as an edge detection method which was proposed by Lam et al. (1992), Kovesi (1997, 1999), Holden et al. (2008), and Holden et al. (2010). In this context, we used a quantitative method that includes three stages:

1) Specifying local neighborhood by the standard deviation (SD). The equation for SD is provided as:

$$SD = \sqrt{\frac{1}{N} \sum (x_i - \mu)^2} \quad (3)$$

where N is the number of data and μ is the mean value of data within the window.

2) Quantitatively detecting lateral continuities or line-like features by frequency-based approach. If

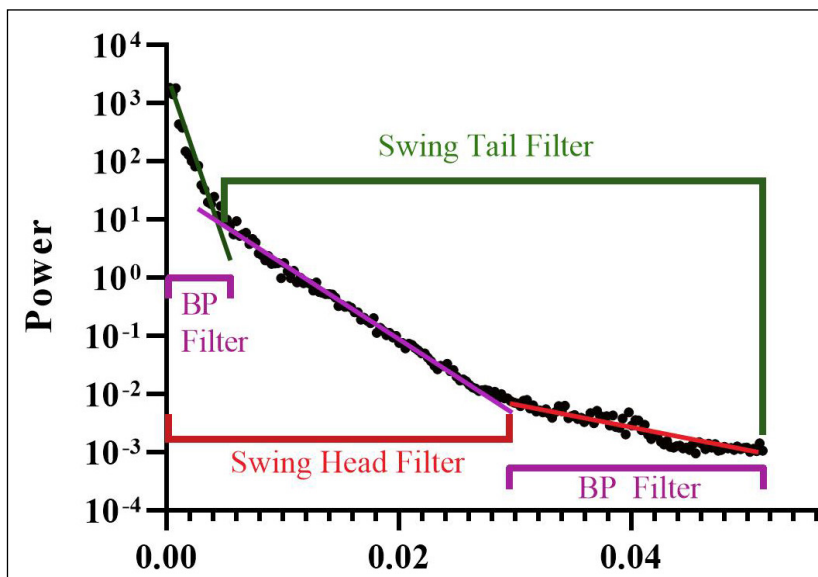


Figure 5- Brief explanation of swing-tail, swing-head, and a band-pass filter (BP filter) on the RAPS.

$r_i(x)$ and $i_i(x)$ considered as real and imaginary parts of the signal and $A_n(x) = \sqrt{r_i(x)^2 + i_i(x)^2}$, symmetry can be computed as:

$$Sym(x) = \frac{\sum_{i=1}^n (|r_i(x)| - |i_i(x)| - T)}{\sum_{i=1}^n A_n(x) + \epsilon} \quad (4)$$

where T is a term for noise suppression and ϵ is used as a constant to prevent division by zero.

3) Skeletonising the discontinuities. First of all, connected edge sets should be constructed. Line segments are fitted to the connected edges. Then, the threshold value is determined. The maximum deviation between the fitted line segment and edge ought to be calculated. If the deviation exceeds the threshold value, the edge is split into two components approximate location of the maximum deviation. This is an iterative process, the maximum deviation is divided into two components until the maximum deviation keeps within the threshold.

4. Findings

RAPS, band-pass filtering, and depth slicing method are applied to the whole study area, western part (area 1), central part (area 2), and eastern part (area 3) of the study area (Figure 1).

The radially averaged depths for the study area, area 1, area 2, and area 3 are estimated by the RAPS. These depths can be considered as approximate depths of the major tectonic sequences. Figure 6 demonstrates the RAPS of the whole study area. Additionally, the RAPS results of area 1, area 2, and area 3 are presented in Figure 7.

As it can be seen from Figure 6, four different primary depth sources are detected. In order to design the appropriate filter, the wavenumber range of

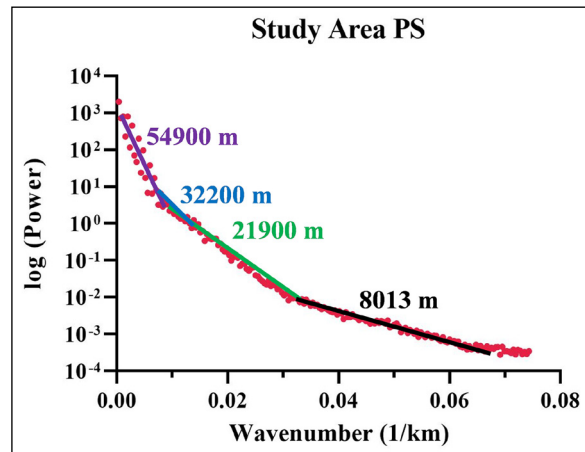


Figure 6- Radially averaged depth values of the whole study area.

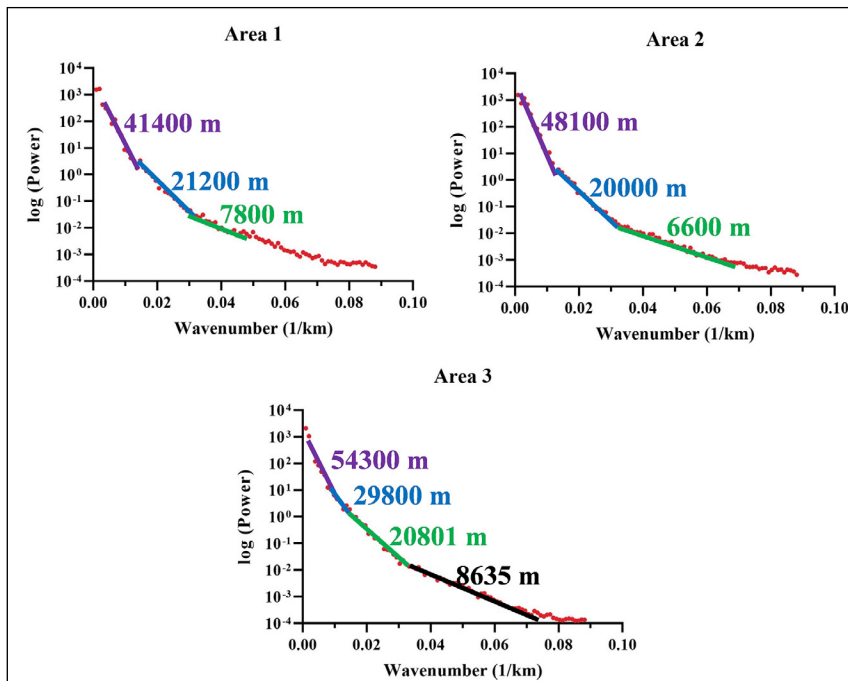


Figure 7- Radially averaged depth values of area 1 (western part), area 2 (central part), and area 3 (eastern part).

each depth source should be detected. The detected approximate wavenumber ranges for the detected depth sources are 0.000-0.010 1/km for 54.9 km, 0.010- 0.012 1/km for 32.2 km, 0.012-0.025 1/km for 21.9 km and 0.025-0.061 1/km for 8 km.

For the area 1, the wavenumber ranges are roughly 0.003-0.013 1/km for 41.4 km, 0.013-0.029 1/km for 21.2 km, 0.029-0.065 1/km for 7.8 km. In the area 2, approximate wavenumber intervals are 0.002-0.013 1/km for 48.1 km, 0.013-0.026 1/km for 20.0 km, 0.026-0.068 1/km for 6.6 km. The selected wavenumber intervals for the area 3 are about 0.001-0.011 1/km for 54.3 km, 0.008-0.011 1/km for 29.8 km, 0.011-0.032 1/km for 20.8 km, 0.032-0.070 1/km for 8.6 km.

The gravity anomaly for the corresponding average depth is obtained after the filtering desired

wavenumber intervals. The filtered gravity anomaly for the whole study area, area 1, area 2, and area 3 are shown in Figures 8, 9, 10, and 11.

The computed edge detection map of the entire study area is demonstrated in Figure 17. Tectonic features and quantitatively interpreted discontinuities are overlaid to the SD map.

5. Qualitative and Quantitative Interpretation

Tectonic boundaries, faults, lineaments overlaid on gravity anomalies. Furthermore, their variations with different radial average depths are interpreted. Firstly, the name and position of the emphasized tectonic features are presented in the study area (Figure 12). Then, the geological structures are overlaid on the whole study area (Figure 13), area 1 (Figure 14),

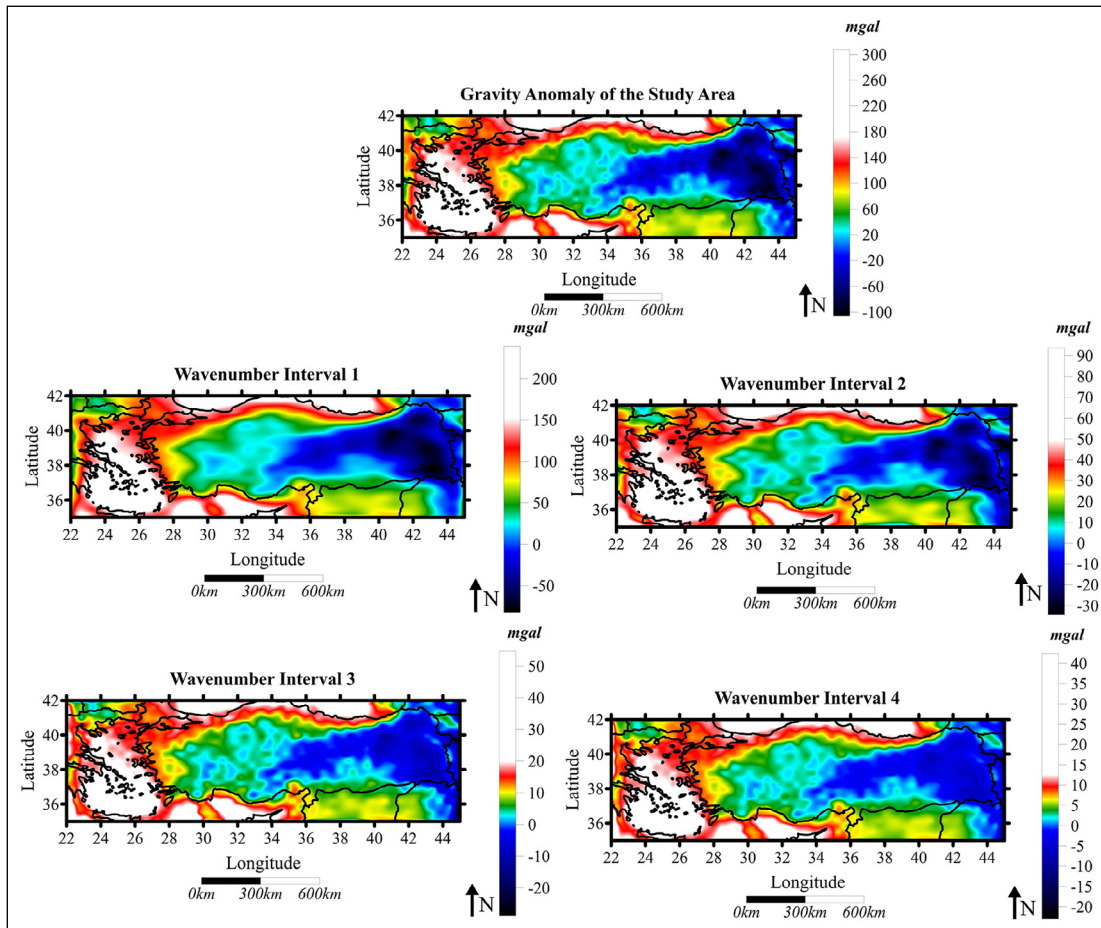


Figure 8- The gravity anomaly of the study area and its filtered components. Wavenumber interval 1 (54.9 km) = 0.000 - 0.010 1/km, wavenumber interval 2 (32.2 km) = 0.010 - 0.012 1/km, wavenumber interval 3 (21.9 km) = 0.012 - 0.025 1/km and wavenumber interval 4 (8 km) = 0.025 - 0.061 1/km.

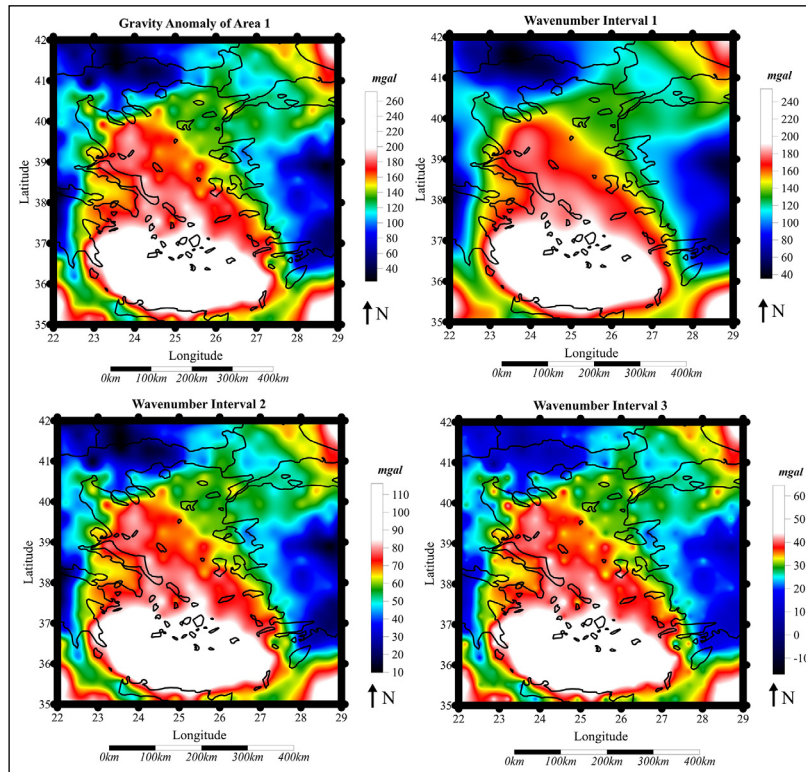


Figure 9- The gravity anomaly of area 1 and its filtered components. wavenumber interval 1 (41.4 km) = 0.003 - 0.013 1/km, wavenumber interval 2 (21.2 km) = 0.013 - 0.029 1/km, wavenumber interval 3 (7.8 km) = 0.029 - 0.065 1/km.

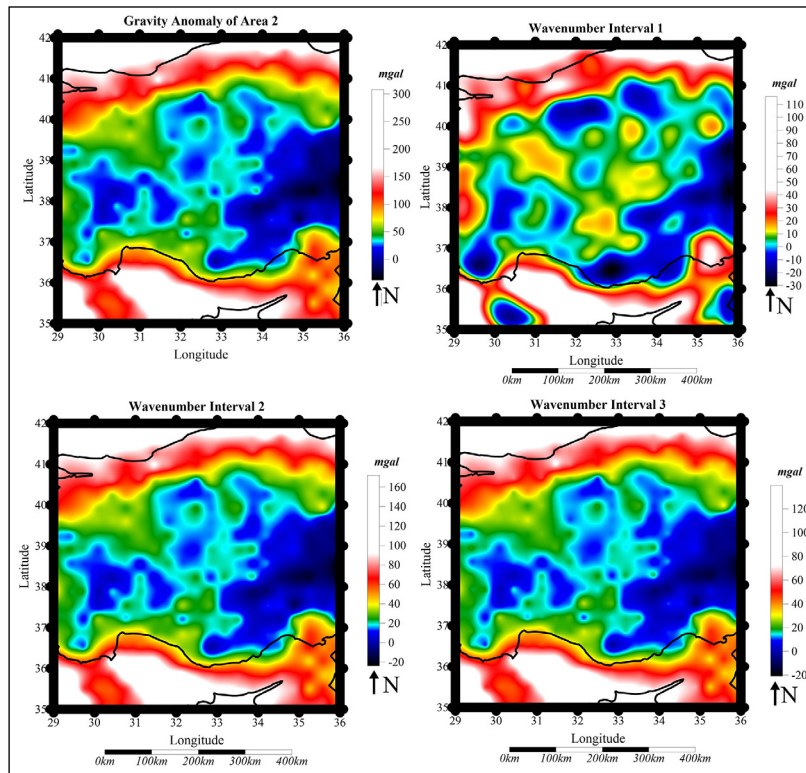


Figure 10- The gravity anomaly of area 3 and its filtered components. Wavenumber interval 1 (48.1 km) = 0.002 - 0.013 1/km, wavenumber interval 2 (20.0 km) = 0.013 - 0.026 1/km, wavenumber interval 3 (6.6 km) = 0.026 - 0.068 1/km.

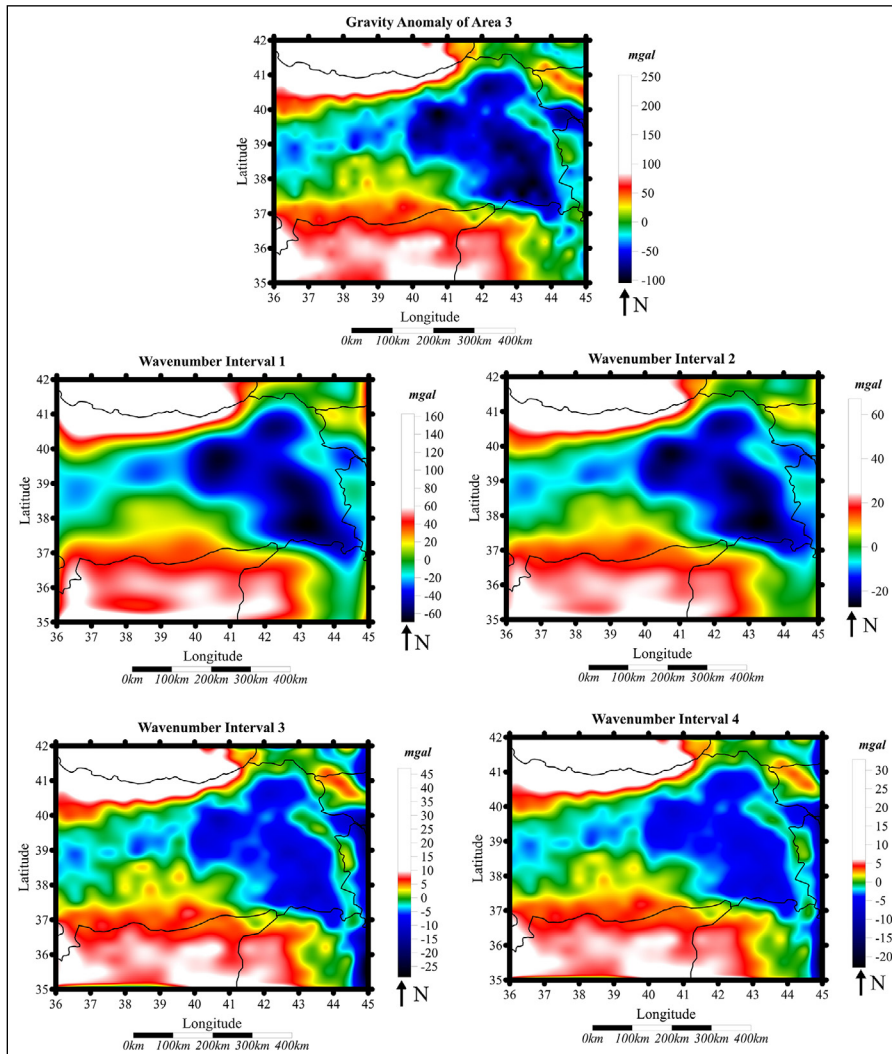


Figure 11- The gravity anomaly of area 3 and its filtered components. Wavenumber interval 1 (54.3 km) = 0.001 - 0.011 1/km, wavenumber interval 2 (29.8 km) = 0.008 - 0.011 1/km, wavenumber interval 3 (20.8 km) = 0.011 - 0.032 1/km, wavenumber interval 4 (8.6 km) = 0.032 - 0.070 1/km.

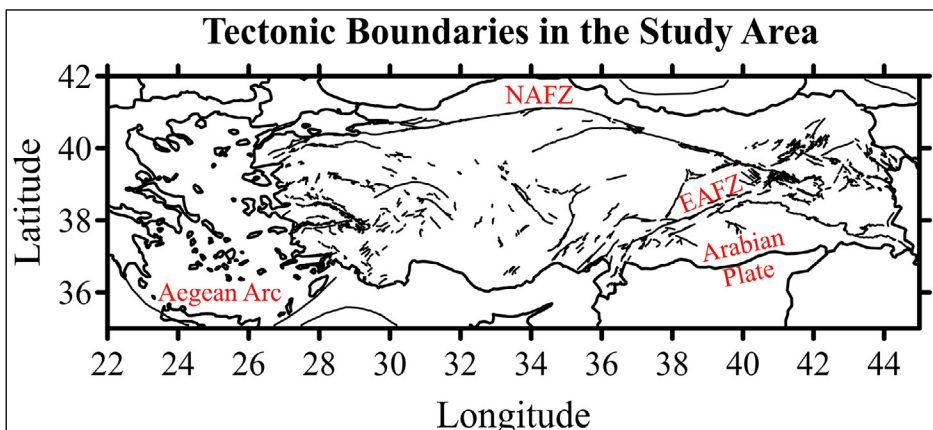


Figure 12- The major tectonic boundaries which are used in the interpretation phase.

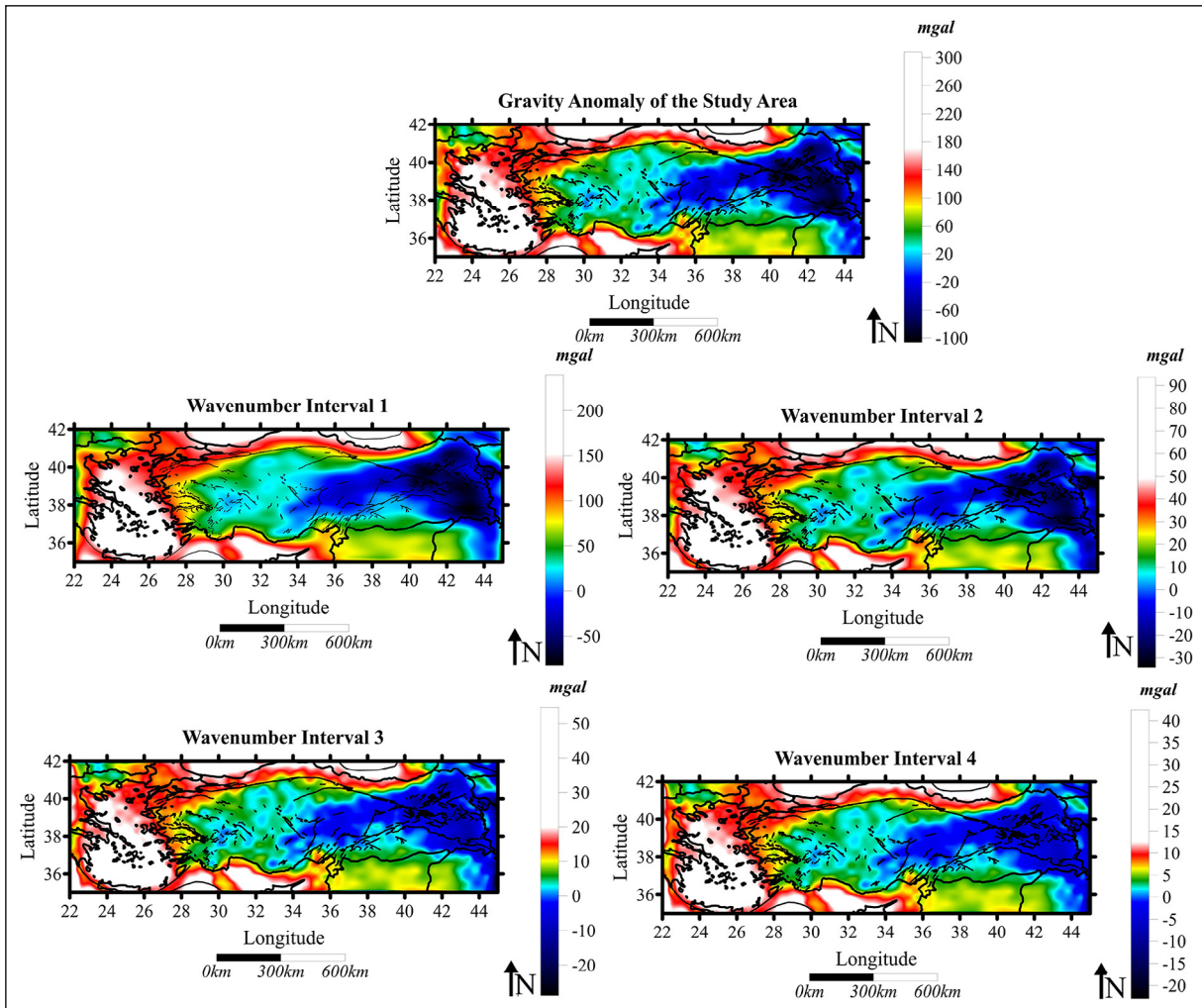


Figure 13- Qualitative interpretation of the whole study area. Wavenumber interval 1 (54.9 km) = 0.000 - 0.010 1/km, wavenumber interval 2 (32.2 km) = 0.010 - 0.012 1/km, wavenumber interval 3 (21.9 km) = 0.012 - 0.025 1/km and wavenumber interval 4 (8 km) = 0.025 - 0.061 1/km.

area 2 (Figure 15), and area 3 (Figure 16) for the detailed analysis.

In Figure 13, the wavenumber interval 1, containing the longest wavelengths, smoothly reflects the deeper geological variations in the study area. On the other hand, wavelength interval 4, which includes the shortest wavelength components, generally presents the shallower tectonic characteristics.

Broadly speaking, the geodynamics of the eastern part is controlled by the deeper mechanisms since the notable decrease in gravity anomaly occurs only for the long-wavelength components (wavenumber interval 1 and wavenumber interval 2). Conversely,

the gravity anomaly of the western part is quite stable for each wavelength component. The central part of the study can be barely interpreted from the regional study area as tectonic structures are quite small with respect to the resolution of data.

Extensional tectonics along the N-S direction dominates Western Anatolia Region. The extensional mechanism results in E-W grabens. Moreover, the subduction zone between the Eurasia Plate and the African Plate formed Aegean Arc.

As it can be seen from Figure 14, the western part of the study area, area 1, is demonstrated. The location of the Aegean Arc is fairly obvious in each

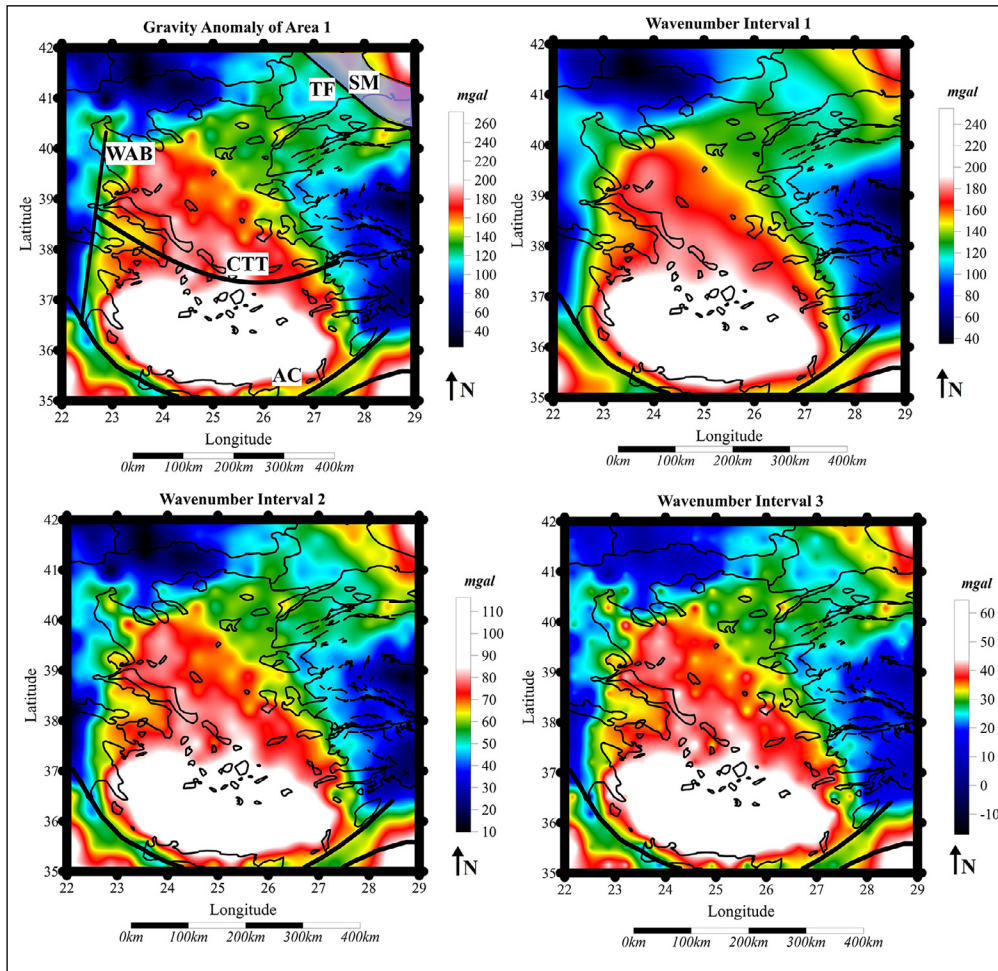


Figure 14- Qualitative interpretation of area 1. Wavenumber interval 1 (41.4 km) = 0.003 - 0.013 1/km, wavenumber interval 2 (21.2 km) = 0.013 - 0.029 1/km, wavenumber interval 3 (7.8 km) = 0.029 - 0.065 1/km. Interpreted tectonic structures are WAB= West Aegean Boundary, TF= Thrace Fault, CTT= Cycladic Tectonic Trend, SM= Strandja Massif.

wavelength interval. This subduction zone, related to the Aegean Arc, is specified by a higher gravity anomaly. Furthermore, it can be said that the Aegean Arc dominates the tectonic mechanism of area 1 for each depth segment.

It is known that accumulated sediments in grabens are generally characterised by a decreasing gravity anomaly. The effect of sedimentation in Western Anatolia can be tracked from the wavenumber interval 3, whose radial average depth is roughly 8 km. In addition, minor faults indicate boundaries of grabens in area 1. Unlike the Aegean Arc, grabens can be associated with the shallow tectonic regime of Western Anatolia.

Thrace Fault can be observed in each depth interval (depth intervals 1, 2, and 3) and its strike is NW-SE. Southwest of the Thrace Fault is characterised by lower gravity anomalies while higher gravity anomalies are observed in the northeast part (Strandja Massif) of the fault. It might be said that the northern Aegean Region and the southern Thrace have fairly similar tectonic characteristics. There is a major boundary that initiated from the southern Aegean plate to the northwestern part of the Aegean Plate where the Thrace fault is discontinuous in the Peloponnese. This major boundary is the crustal-scale and it can be interpreted from each depth interval.

Notably high gravity anomaly zone is bounded by Crete Island in the south and Cyclades Massif in the

north. Moreover, subduction of the African plate to the Aegean Plate formed fore-arc structures which are characterized by lower gravity anomalies.

In general, the shallow and extensional tectonic regime in the Western Anatolia demonstrates credible similarities with previous studies (Sarı et al., 2002; Tirel et al., 2004; Pamukçu and Yurdakul, 2008; Doğru et al., 2017, 2018; Kahveci et al., 2019; Doğru and Pamukçu, 2019).

In Figure 15, Aegean Arc and NAFZ are the major tectonic structures. The edge of the Aegean Arc cannot be clearly observed in the deepest depth slice (wavenumber interval 1 (48.1 km)) whereas its boundaries are more obvious in wavenumber interval 2 (20.0 km) and wavenumber interval 3 (6.6 km). The position of the NAFZ is considerably obvious in each pseudo-depth segment. Therefore, it can be said that NAFZ has an impact at each radial average depth, 48.1 km, 20 km, and 6.6 km. Overall, gravity anomalies

in each depth segment are quite stable from deeper to shallower in Central Anatolia.

Even though NAFZ adversely correlated to the plate boundaries in the East, it is quite concordant with the boundary of the western Pontides. In this case, it might be said that NAFZ becomes deeper from the East to the West. Salt Lake fault is not corresponding to the gravity anomalies. Therefore, it can be said that this fault formed in shallow depths.

In the Antalya region, there is an anomaly along the NW direction, which is possibly associated with boundary transition. Both sides of the Antalya-Samsun lineament (wavenumber intervals 1, 2, and 3) can be characterised by different crustal thicknesses. The change in crustal thickness formed three tectonic sub-regions.

Thrace-Eskişehir fault zone along NW direction is correlated with gravity anomalies in-depth interval 1.

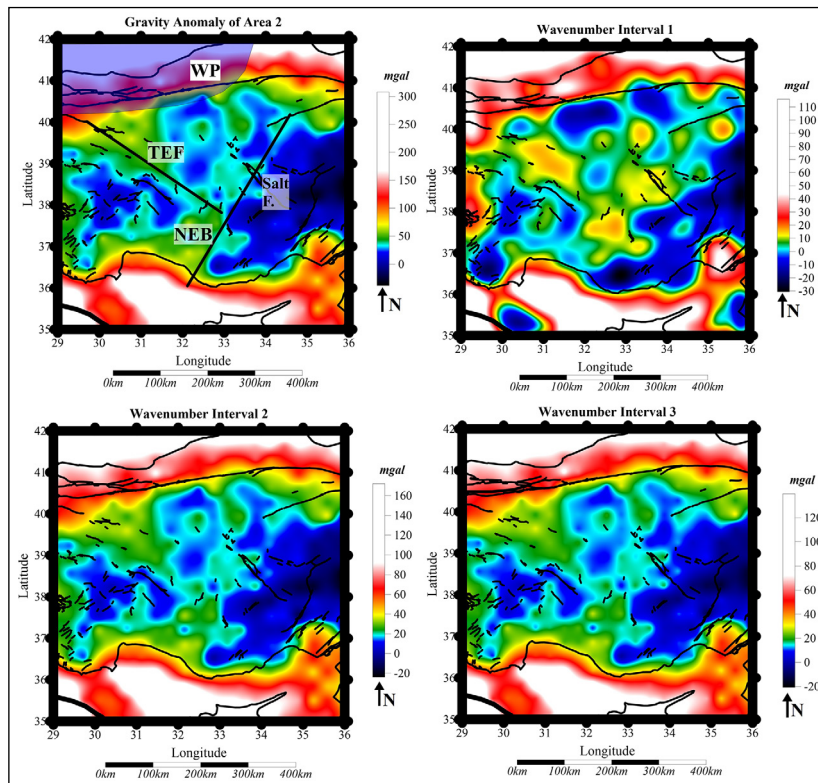


Figure 15- Qualitative interpretation of area 2. Wavenumber interval 1 (48.1 km) = 0.002-0.013 1/km, wavenumber interval 2 (20.0 km) = 0.013-0.026 1/km, wavenumber interval 3 (6.6 km) = 0.026-0.068 1/km. Interpreted tectonic structures are WP= Western Pontides, TEF= Thrace-Eskişehir Fault, NEB= Northeast Boundary, Salt F.= Salt Lake Fault.

Plate shortening initiated from the southern Cyprus region can be tracked to the Mersin-Anamur shoreline while it cannot be observed across the Antalya-İskenderun shoreline.

The interpreted tectonic structures and discontinuities in Central Anatolia is somewhat correlated with regional scale gravity anomalies (Büyüksaraç et al., 2005; Önal et al., 2008; Oruç, 2011, Bilim et al., 2017, Bilim, 2017 and Oruç et al., 2019).

The dominant tectonic mechanism in Eastern Anatolia is the compressional regime. Minor faults in Eastern Anatolia are related to the continental collision. The lower gravity anomaly in area 3 can be associated with the regions with crustal thickening (Figure 16). Lower gravity anomalies were observed where NAFZ and EAFZ coincided. There is no significant variation on the gravity anomaly within the Arab Platform due to the stable tectonic characteristics of this platform.

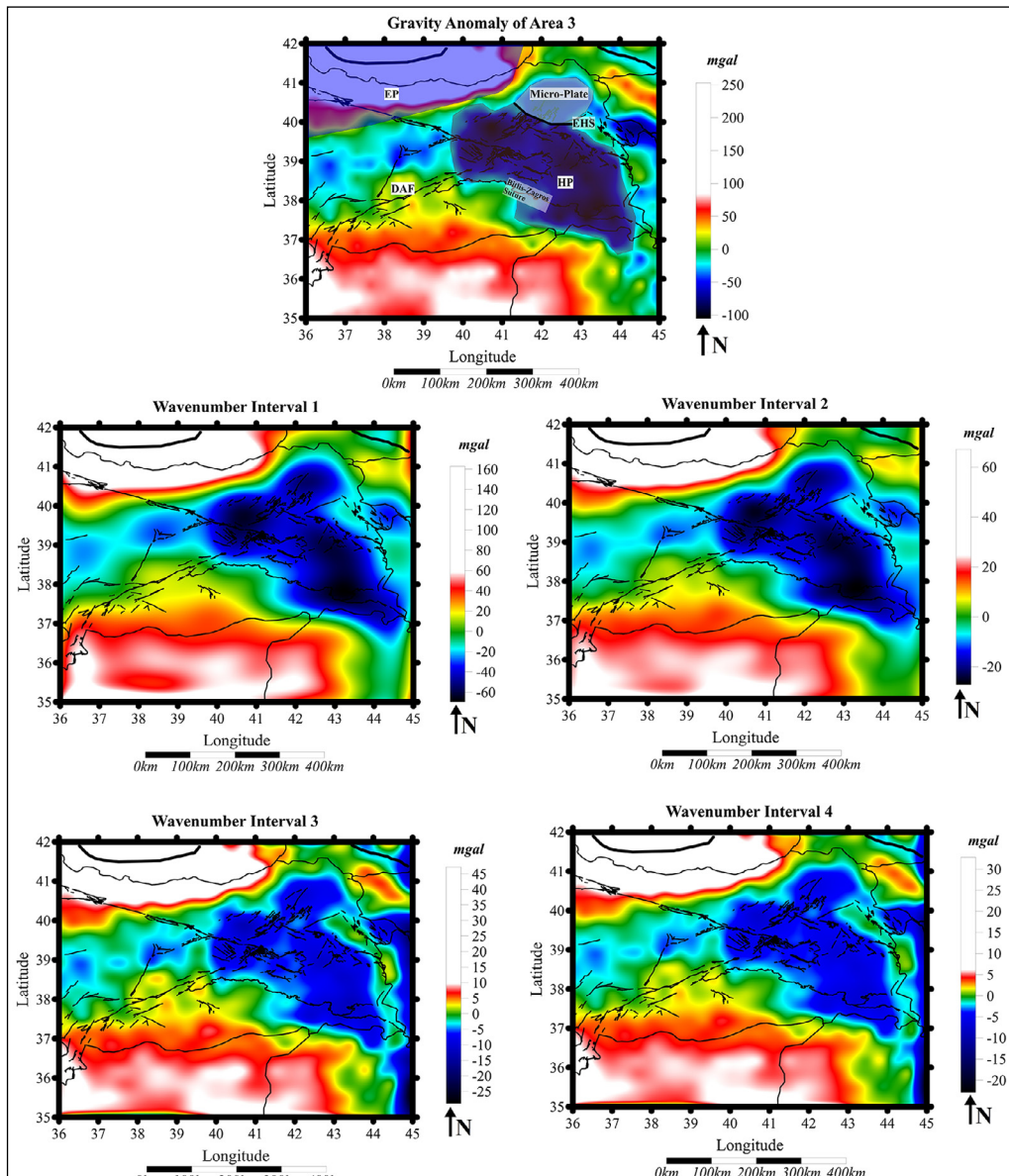


Figure 16- Qualitative interpretation of area 3. Wavenumber interval 1 (54.3 km) = 0.001 - 0.011 1/km, wavenumber interval 2 (29.8 km) = 0.008 - 0.011 1/km, wavenumber interval 3 (20.8 km) = 0.011 - 0.032 1/km, wavenumber interval 4 (8.6 km) = 0.032 - 0.070 1/km. Interpreted tectonic structures are; EP= Eastern Pontides, DAF= East Anatolian Fault, HP= Hakkari Plate, EHS= Erzurum -Horasan Subsidence.

If gravity anomalies in Figure 16 are analyzed in terms of various depth segments, the effect of crustal thickening, minor faults, and boundaries of the Arabian Platform are becoming uncertain with decreasing radial average depth. Interpretation of the minor fault zone can be conducted by the longer wavelength components, wavenumber interval 1 (54.3 km) and wavenumber interval 2 (29.8 km). The minor fault zone was barely detected from the shorter wavelength components, wavenumber interval 3 (20.8 km) and wavenumber interval 4 (8.6 km), owing to the fact that this zone occurred at deeper parts of the subsurface.

Eastern Pontide, Eastern Anatolia, and the northern part of the Eastern Anatolia (microplate) are three major plate boundaries in area 3. The microplate (area 3) is bounded by Erzurum-Horasan subsidence in the Southwest and the national border of Türkiye in the east. Furthermore, the boundaries of the Hakkari plate are; southern part of the Türkiye-Iraq national border in the south, the Türkiye-Iran national border in the east, the Erzurum-Horasan subsidence in the north, and the Arabian plate in the west. The EAFZ and the Arabian Plate can be interpreted in all depth intervals and the gravity anomaly. EAFZ is concordant with

tectonic structures in each depth interval whereas NAFZ cannot be correlated with deeper tectonic structures. This concordance might be tracked from the following previous studies: Pamukçu et al. (2007), Büyüksaraç (2007), Maden et al. (2009) and Pamukçu et al. (2015). The tectonic boundaries in Eastern Anatolia resulted from the northward movement of the Arabian plate.

The interpreted tectonic boundaries and discontinuities for the whole study area are somewhat compatible with Ateş et al., (2012). The major difference between Ateş et al., (2012) and this study is the resolution of the gravity data. Since WGM 2012 resolution is not as high as interpreted gravity data in Ateş et al. (2012), minor discontinuities are unlikely to be interpreted.

For the purpose of obtaining an unbiased interpretation of the study area, a quantitative edge detection method is used. The detected discontinuities are compared to the tectonic features in the study area (Figure 17). Initially, it is worth saying that the land-marine transition zones generated dramatically high contrast in the SD map. Therefore, the edge detection technique assigned linear features to these zones.

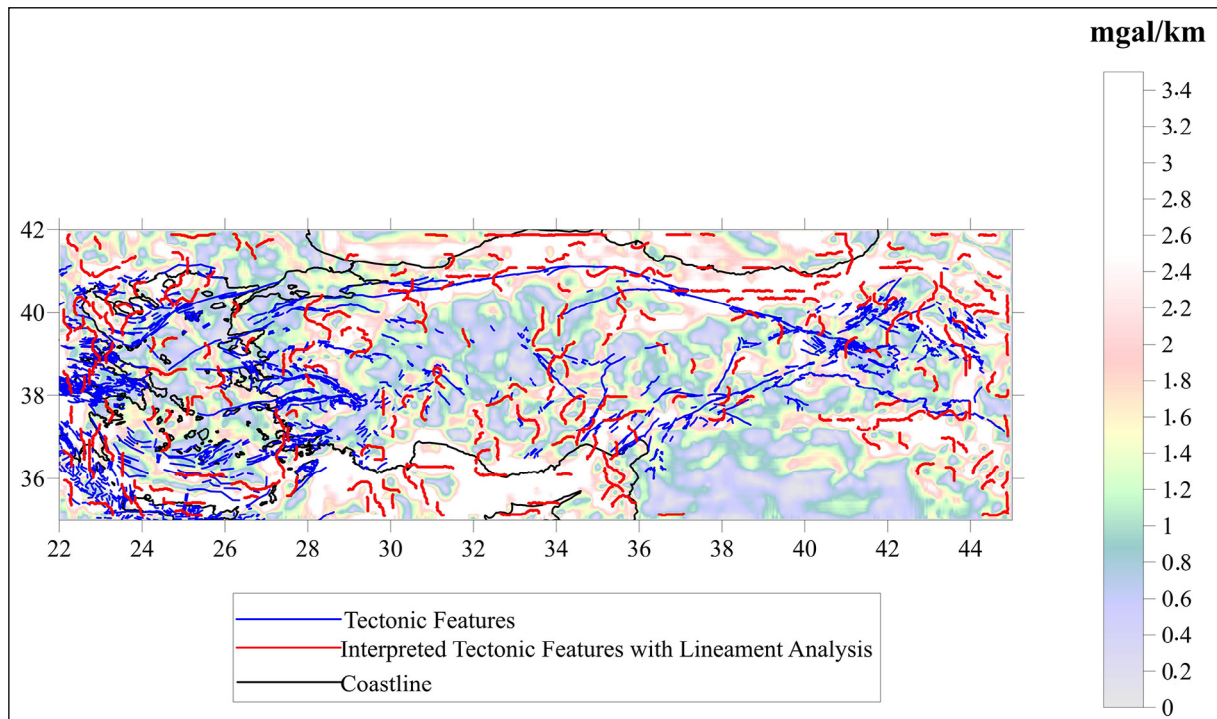


Figure 17- Standard deviation map which is overlaid by tectonic features (blue) and interpreted lineaments (red).

In the western part of the study area, lineaments are more or less correlated with geological structures except for Western Anatolia. The graben structures in Western Anatolia produce non-symmetrical anomalies and edge detection methods unable to detect these structures. However, this problem might be overcome using data with higher resolution. Furthermore, the detected linear features and geological discontinuities are compatible in Central Anatolia. It is fair to say that NAFZ is credibly interpreted by the quantitative approach. In Eastern Anatolia, the Arabian platform is barely detected due to the lower contrast and symmetry in the SD anomaly. Nevertheless, the tectonic features in Northeast Anatolia somewhat reliably correspond to the estimated linear segments.

6. Results

Interpretation of the study area for different pseudo-depth segments described variation of tectonic elements with depth. The method combined the results of the radial average power spectrum and band-pass filter. This study provided a different perspective of interpretation which takes into account depth dimension simultaneously.

From the West to the East, dominant tectonic events occurred shallower to deeper subsurface. Grabens have a quite clear gravity anomaly at only the shallowest depth (≈ 8 km) in Western Anatolia. In addition, the crustal thickening effect can be observed at deeper parts (≈ 54.3 and ≈ 29.8 km) of the subsurface in Eastern Anatolia. NAFZ is the major structure that is interpretable at each pseudo-depth segment.

The qualitatively interpreted discontinuities are compared to the line segments obtained from the quantitative edge detection method. The comparison results are not presenting a perfect correlation but credible interpretation might be achieved. Although quantitative and automated edge detection methods provide notably precise findings, the accuracy of these approaches is not as high as the precision. As a consequence, the combination of qualitative and quantitative techniques would yield better interpretation.

Regarding the limitations of this study, it is apparent that WGM 2012 gravity anomaly is dominated by the

longer wavelength components. Shorter wavelength components cannot be analyzed due to the dominant high-altitude measurements. Therefore, the RAPS results barely detect shorter wavelength components. The second limitation is that the determination of the pseudo-depth segments from RAPS is quite subjective.

Acknowledgements

We would like to express our sincere thanks to anonymous reviewers for their constructive comments.

References

- Altuner, D., Koçyiğit, A. 1993. Third remark on the geology of Karakaya basin. An Anisian mega block in northern Central Anatolia: micropaleontologic, stratigraphic and tectonic implications for the rifting stage of Karakaya basin, Turkey. *Revue De Paléobiologie* 12(1), 1-17.
- Altuner, D., Koçyiğit, A., Farinacci, A., Nicosia, U., Conti, M. A. 1991. Jurassic, lower Cretaceous stratigraphy and paleogeographic evolution of the southern part of north-western Anatolia. *Geologica Romana* 28, 13-80.
- Amante, C., Eakins, B. W. 2009. ETOPO1 1 arc - minute global relief model: procedures, data sources, and analysis. National Oceanic and Atmospheric Administration Technical Memorandum, NESDIS NGDC-24.
- Arfaoui, M., Inoubli, M. H., Tlig, S., Alouani, R. 2011. Gravity analysis of salt structures: an example from the El Kef - Ouargha region (northern Tunisia). *Geophysical Prospecting* 59(3), 576-591.
- Arslan, S. 2016. Geophysical regional gravity map of Turkey and its general assessment. *Bulletin of the Mineral Research and Exploration* 153, 185-202.
- Ateş, A., Kearey, P., Tufan, S. 1999. New gravity and magnetic anomaly maps of Turkey. *Geophysical Journal International* 136(2), 499-502.
- Ateş, A., Bilim, F., Büyüksaraç, A., Aydemir, A., Bektaş, O., Aslan, Y. 2012. Crustal structure of Turkey from aeromagnetic, gravity and deep seismic reflection data. *Surveys in Geophysics* 33(5), 869-885.
- Aydın, M., Şahintürk, Ö., Serdar, H. S., Özçelik, Y., Akarsu, I., Üngör, A., Çokuğraş, R., Kasar, S. 1986. Ballıdağ - Çangaldağ (Kastamonu) arasındaki bölgenin jeolojisi. *Geological Society of Turkey Bulletin* 29, 1-16.

- Bhattacharyya, B. K. 1966. Continuous spectrum of the total - magnetic - field anomaly due to a rectangular prismatic body. *Geophysics* 31(1), 97-121.
- Bilim, F. 2017. Investigating Moho depth, Curie point, and heat flow variations of the Yozgat Batholith and its surrounding area, north-central Anatolia, Turkey, using gravity and magnetic anomalies. *Turkish Journal of Earth Sciences* 26(6), 410-420.
- Bilim, F., Koşaroglu, S., Aydemir, A., Büyüksaraç, A. 2017. Thermal investigation in the Cappadocia Region, central Anatolia - Turkey, analyzing Curie point depth, geothermal gradient, and heat-flow maps from the aeromagnetic data. *Pure and Applied Geophysics* 174(12), 4445-4458.
- Bingöl, E., Akyürek, B., Korkmazer, B. 1975. Geology of the Biga Peninsula and some characteristics of the Karakaya Formation. Congress of Earth Sciences on the Occasion of the 50th Anniversary of the Turkish Republic. Maden Teknik Arama Genel Müdürlüğü, Ankara, 71-77.
- Bonvalot, S., Balmino, G., Briais, A., Kuhn, M., Peyrefitte, A., Vales, N., Biancale, R., Gabalda, G., Reinquin, F. 2012. World gravity map: a set of global complete spherical Bouguer and isostatic anomaly maps and grids. European Geosciences Union General Assembly, 11091.
- Bozkurt, E., Mittwede, S. K. 2001. Introduction to the geology of Turkey - a synthesis. *International Geology Review* 43(7), 578-594.
- Büyüksaraç, A. 2007. Investigation into the regional wrench tectonics of inner East Anatolia (Türkiye) using potential field data. *Physics of the Earth and Planetary Interiors* 160(1), 86-95.
- Büyüksaraç, A., Jordanova, D., Ateş, A., Karloukovski, V. 2005. Interpretation of the gravity and magnetic anomalies of the Cappadocia region, central Turkey. *Pure and Applied Geophysics* 162(11), 2197-2213.
- Cattò, S., Cavazza, W., Zattin, M., Okay, A. I. 2018. No significant Alpine tectonic overprint on the Cimmerian Strandja Massif (SE Bulgaria and NW Turkey). *International Geology Review* 60(4), 513-529.
- Cordell, L., Grauch, V. J. S. 1985. Mapping basement magnetization zones from aeromagnetic data in the San Juan Basin, New Mexico in the utility of regional gravity and magnetic anomaly maps. *Society of Exploration Geophysicists*, 181-197.
- Dean, W. T., Monod, O., Rickards, R. B., Demir, O., Bultynck, P. 2000. Lower Palaeozoic stratigraphy and palaeontology, Karadere – Zirze area, Pontus mountains, northern Turkey. *Geological Magazine* 137(5), 555-582.
- Dewey, J. F., Hempton, M. R., Kidd, W. S. F., Saroğlu, F., Şengör, A. M. C. 1986. Shortening of continental lithosphere: the neotectonics of Eastern Anatolia - a young collision zone. *Geological Society Special Publication* 19(1), 1-36.
- Doğru, F., Pamukçu, O. 2019. Analysis of gravity disturbance for boundary structures in the Aegean Sea and western Anatolia. *Geofizika* 36(1), 53-76.
- Doğru, F., Pamukçu, O., Özsoz, I. 2017. Application of tilt angle method to the Bouguer gravity data of western Anatolia. *Bulletin of the Mineral Research and Exploration* 2017(155), 213-222.
- Doğru, F., Pamukçu, O., Gönenç, T., Yıldız, H. 2018. Lithospheric structure of western Anatolia and the Aegean Sea using GOCE - based gravity field models. *Bollettino Di Geofisica Teorica Ed Applicata* 59(2), 135-160.
- Durand, B., Jolivet, L., Horvath, F., Seranne, M. 1999. The Mediterranean Basins: Tertiary extension within the Alpine Orogen. *Geological Society of London* 156.
- Elmas, A., Yiğitbaş, E. 2001. Ophiolite emplacement by strike-slip tectonics between the Pontide Zone and the Sakarya Zone in northwestern Anatolia, Turkey. *International Journal of Earth Sciences* 90(2), 257-269.
- Erdoğan, B. 1990. Stratigraphy and tectonic evolution of the İzmir - Ankara Zone between İzmir - Seferihisar. *Turkish Association Petroleum Geology* 2, 1-20.
- Fairhead, J. D. 2016. *Advances in Gravity and Magnetic Processing and Interpretation*. European Association of Geoscientists and Engineers Publications.
- Faccenna, C., Bellier, O., Martinod, J., Piromallo, C., Regard, V. 2006. Slab detachment beneath eastern Anatolia: a possible cause for the formation of the North Anatolian Fault. *Earth and Planetary Science Letters* 242(1-2), 85-97.
- Genç, Ş. C., Yılmaz, Y. 1995. Evolution of the Triassic continental margin, Northwest Anatolia. *Tectonophysics* 243(2), 193-207.
- Göğüş, O. H., Psyklywec, R. N. 2008. Mantle lithosphere delamination driving plateau uplift and syn-convergent extension in eastern Anatolia. *Geology* 36(9), 723-726.

- Gottlieb, D., Shu, C. W. 1997. On the Gibbs phenomenon and its resolution. *Society for Industrial and Applied Mathematics Review* 39(4), 644-668.
- Göncüoğlu, M. C. 2010. Introduction to the geology of Turkey: geodynamic evolution of the Pre - Alpine and Alpine terranes. *Mineral Research and Exploration Monography Series* 5, 1-69.
- Göncüoğlu, M. C., Turhan, N., Şentürk, K., Özcan, A., Uysal, Ş., Yalınız, M. K. 2000. A geotraverse across northwestern Turkey: tectonic units of the central Sakarya region and their tectonic evolution. *Geological Society of London. Special Publications* 173(1), 139-161.
- Görür, N., Monod, O., Okay, A.I., Şengör, A. M. C., Tüysüz, O., Yiğitbaş, E., Sakiñ, M., Akkök, R. 1997. Palaeogeographic and tectonic position of the Carboniferous rocks of the western Pontides (Turkey) in the frame of the Variscan belt. *Bulletin De La Société Géologique de France* 168(2), 197-205.
- Görür, N., Tüysüz, O., Şengör, A. M. C. 1998. Tectonic evolution of the central Anatolian basins. *International Geology Review* 40(9), 831-850.
- Görür, N., Çağatay, N., Sakiñ, M., Akkök, R., Tchapylyga, A., Natalin, B. 2000. Neogene Paratethyan succession in Turkey and its implications for the paleogeography of the Eastern Paratethys. *Geological Society of London. Special Publications* 173(1), 251-269.
- Gülyüz, E., Özkaptan, M., Kaymakçı, N., Persano, C., Stuart, F. M. 2019. Kinematic and thermal evolution of the Haymana basin, a fore-arc to a foreland basin in central Anatolia (Turkey). *Tectonophysics* 766, 326-339.
- Gupta, V. K., Ramani, N. 1980. Some aspects of regional - residual separation of gravity anomalies in a Precambrian terrain. *Geophysics* 45(9), 1412-1426.
- Harris, N. B., Kelley, S., Okay, A. I. 1994. Post-collision magmatism and tectonics in northwest Anatolia. *Contributions to Mineralogy and Petrology* 117(3), 241-252.
- Holden, E. J., Dentith, M., Kovesi, P. 2008. Towards the automated analysis of regional aeromagnetic data to identify regions prospective for gold deposits. *Computers and Geosciences* 34(11), 1505-1513.
- Holden, E. J., Kovesi, P., Dentith, M. C., Wedge, D., Wong, J. C., Fu, S. C. 2010. Detection of regions of structural complexity within aeromagnetic data using image analysis. *International Conference Image and Vision Computing New Zealand*, 1-8.
- Kahveci, M., Çırmık, A., Doğru, F., Pamukçu, O., Gönenç, T. 2019. Subdividing the tectonic elements of Aegean and Eastern Mediterranean with gravity and GPS data. *Acta Geophysica* 67(2), 491-500.
- Karig, D. E., Kozlu, H. 1990. Late Palaeogene - Neogene evolution of the triple junction region near Maraş, south - central Turkey. *Journal of the Geological Society* 147(6), 1023-1034.
- Kaymakçı, N., White, S. H., Van Dijk, P. M. 2000. Palaeostress inversion in a multiphase deformed area: kinematic and structural evolution of the Çankırı Basin (Central Türkiye), part 1- northern area. *Geological Society of London. Special Publications* 173(1), 295-323.
- Keskin, M. 2007. Eastern Anatolia: a hotspot in a collision zone without a mantle plume. *Special Paper of the Geological Society of America* 430, 693-722.
- Ketin, İ. 1966. Tectonic units of Anatolia (Asia minor). *Bulletin of the Mineral Research and Exploration* 66, 66.
- Ketin, I. 1969. About the North Anatolian Fault. *Bulletin Mineral Research and Exploration Institute Turkey* 72, 1-29.
- Koçyiğit, A. 1987. Tectono-stratigraphy of the Hasanoğlan (Ankara) region: evolution of the Karakaya orogen. *Yerbilimleri* 14, 269-293.
- Koçyiğit, A. 1991. First remarks on the geology of the Karakaya Basin: Karakaya orogen and Pre-Jurassic nappes in eastern Pontides, Turkey. *Geologica Romana* 27, 3-11.
- Kovesi, P. 1997. Symmetry and asymmetry from the local phase. In *Tenth Australian Joint Conference on Artificial Intelligence* 190, 2-4.
- Kovesi, P. 1999. Image features from phase congruency. *Journal of Computer Vision Research* 1(3), 1-26.
- Kozur, H. W., Aydın, M., Demir, O., Yakar, H., Göncüoğlu, M. C., Kuru, F. 2000. New stratigraphic and palaeogeographic results from the Palaeozoic and early Mesozoic of the Middle Pontides (northern Turkey) in the Azdavay, Devrekani, Küre, and Inebolu areas: implications for the Carboniferous - Early Cretaceous geodynamic evolution and some related remarks to the Karakaya oceanic rift basin. *Geologia Croatica* 53(2), 209-268.
- Lam, L., Lee, S. W., Suen, C. Y. 1992. Thinning methodologies - a comprehensive survey. *Institute*

- of Electrical and Electronics Engineers 14(9), 869-885.
- Legeay, E., Ringenbach, J. C., Kergaravat, C., Callot, J. P., Mohn, G., Kavak, K. 2016. Geodynamics of the Sivas Basin (Turkey): from a forearc basin to a retro arc foreland basin. European Geosciences Union General Assembly, EPSC2016, 14961.
- Maden, N., Gelisli, K., Eyüboğlu, Y., Bektaş, O. 2009. Determination of the tectonic and crustal structure of the eastern pontide orogenic belt (NE Turkey) using gravity and magnetic data. Pure and Applied Geophysics 166(12), 1987-2006.
- Mallick, K., Sharma, K. K. 1999. A finite element method for computation of the regional gravity anomaly. Geophysics 64(2), 461-469.
- Maus, S., Dimri, V. 1995. Potential field power spectrum inversion for scaling geology. Journal of Geophysical Research: Solid Earth 100(B7), 12605-12616.
- Moix, P., Beccaletto, L., Kozur, H. W., Hochard, C., Rosselet, F., Stampfli, G. M. 2008. A new classification of the Turkish terranes and sutures and its implication for the paleotectonic history of the region. Tectonophysics 451(1-4), 7-39.
- Ocakoğlu, F. 2001. Repetitive subtidal - to - coastal sabkha cycles from a Lower - Middle Miocene marine sequence, eastern Sivas Basin. Turkish Journal of Earth Sciences 10(1), 17-34.
- Okay, A. I. 1989. Tectonic units and sutures in the Pontides, northern Turkey. In tectonic evolution of the Tethyan region. Springer, Dordrecht, 109-116.
- Okay, A. I., Monié, P. 1997. Early Mesozoic subduction in the eastern Mediterranean: evidence from Triassic eclogite in northwest Turkey. Geology 25(7), 595-598.
- Okay, A. I. Tüysüz, O. 1999. Tethyan sutures of northern Turkey. Geological Society of London. Special Publications 156(1), 475-515.
- Okay, A. I., Şengör, A. C. M., Görür, N. 1994. Kinematic history of the opening of the Black Sea and its effect on the surrounding regions. Geology 22(3), 267-270.
- Okay, A. I., Tansel, I., Tüysüz, O. 2001. Obduction, subduction, and collision as reflected in the Upper Cretaceous - Lower Eocene sedimentary record of western Turkey. Geological Magazine 138(2), 117-142.
- Oruç, B. 2011. Edge detection and depth estimation using a tilt angle map from gravity gradient data of the Kozaklı - central Anatolia region, Turkey. Pure and Applied Geophysics 168(10), 1769-1780.
- Oruç, B., Ulutaş, E., Pamukçu, O., Selim, H. H., Sönmez, T. 2019. Rheological stratification and spatial variations in the effective elastic thickness of the lithosphere underneath the central Anatolian region, Turkey. Journal of Asian Earth Sciences 176, 1-7.
- Önal, K. M., Büyüksaraç, A., Aydemir, A., Ateş, A. 2008. Investigation of the deep structure of the Sivas Basin (inner east Anatolia, Turkey) with geophysical methods. Tectonophysics 460(1-4), 186-197.
- Özcan, A., Göncüoğlu, M. C., Turan, N., Uysal, S., Şentürk, K., Isik, A. 1988. Late Palaeozoic evolution of the Kütahya - Bolkağaç belt: Turkey. Middle East Technical University 21, 211-220.
- Özgül, N. 1976. Toroslar'ın bazı temel jeoloji özellikleri. Bulletin of the Geological Society of Turkey 19, 65-78.
- Özgül, N. 1985. Geology of the Alanya region. International Ketin Symposium, Geological Society of Turkey Publication, Ankara, 97-120.
- Pamukçu, O. A., Akçığ, Z., Demirbaş, Ş., Zor, E. 2007. Investigation of crustal thickness in eastern Anatolia using gravity, magnetic and topographic data. Pure and Applied Geophysics 164(11), 2345-2358.
- Pamukçu, O., Yurdakul, A. 2008. Isostatic compensation in Western Anatolia with an estimate of the effective elastic thickness. Turkish Journal of Earth Sciences 17(3), 545-557.
- Pamukçu, O., Gönenç, T., Yurdakul Çırmık, A., Demirbaş, Ş., Tosun, S. 2015. Vertical and horizontal analysis of crustal structure in Eastern Anatolia region. Bulletin of the Mineral Research and Exploration 151, 217-229.
- Pawlowski, R. S., Hansen, R. O. 1990. Gravity anomaly separation by Wiener filtering. Geophysics 55(5), 539-548.
- Robertson, A. 2004. Development of concepts concerning the genesis and emplacement of Tethyan ophiolites in the Eastern Mediterranean and Oman regions. Earth-Science Reviews 66(4), 331-387.
- Robertson, A., Shallo, M. 2000. Mesozoic - Tertiary tectonic evolution of Albania in its regional eastern Mediterranean context. Tectonophysics 316(4), 197-254.
- Robertson, A., Karamata, S., Šarić, K. 2009. Overview of ophiolites and related units in the Late Palaeozoic - Early Cenozoic magmatic and tectonic development of Tethys in the northern part of the Balkan region. Lithos 108(4), 1-36.

- Rojay, B., Altner, D. 1998. Middle Jurassic - Lower Cretaceous biostratigraphy in the Central Pontides (Turkey): remarks on paleogeography and tectonic evolution. *Rivista Italiana di Paleontologia e Stratigrafia* 104(2).
- Rotstein, Y. 1984. Counterclockwise rotation of the Anatolian block. *Tectonophysics* 108(2), 71-91.
- Saramaeki, T., Mitra, S. K., Kaiser, J. F. 1993. Finite impulse response filter design. *Handbook for digital signal processing* 4, 155-277.
- Sarı, C., Şalk, M. 2002. Analysis of gravity anomalies with hyperbolic density contrast: An application to the gravity data of western Anatolia disaster-resilient cities view project analysis of gravity anomalies with hyperbolic density contrast: an application to the gravity data of Western Anatolia. *International Journal of the Balkan Geophysical Society* 5, 3.
- Şaroğlu, F., Yılmaz, Y. 1986. Geological evolution and basin models during a neotectonic episodes in Eastern Anatolia. *Bulletin of the Mineral Research and Exploration* 107, 107.
- Şengör, A. M. C. 1979. Mid - Mesozoic closure of Permo - Triassic Tethys and its implications. *Nature* 279, 590-593.
- Şengör, A. M. C. 1984. The Cimmeride orogenic system and the tectonics of Eurasia. *Geological Society of America Special* 195, 82.
- Şengör, A. M. C. 1987. Tectonics of the Tethysides: orogenic collage development in a collisional setting. *Annual Review of Earth and Planetary Sciences* 15(1), 213-244.
- Şengör, A. M. C., Yılmaz, Y. 1981. Tethyan evolution of Turkey: a plate tectonic approach. *Tectonophysics* 75(4), 181-241.
- Şengör, A. M. C., Kidd, W. S. F. 1979. Post-collisional tectonics of the Turkish - Iranian plateau and a comparison with Tibet. *Tectonophysics* 55(3-4), 361-376.
- Şengör, A. M. C., Yılmaz, Y., Ketin, I. 1980. Remnants of a pre-Late Jurassic ocean in northern Turkey: fragments of Permian-Triassic Paleo-Tethys. *Geological Society of America Bulletin* 91(10), 599-609.
- Şengör, A. M. C., Görür, N., Şaroğlu, F., Biddle, K. T., Christie Blick, N. 1985. Strike-slip deformation, basin formation, and sedimentation. *Society of Economic Palaeontologists and Mineralogists. Special Publication* 37, 227-264.
- Sherlock, S., Kelley, S., Inger, S., Harris, N., Okay, A. 1999. ⁴⁰Ar - ³⁹Ar and Rb - Sr geochronology of high-pressure metamorphism and exhumation history of the Tavşanlı Zone, NW Turkey. *Contributions to Mineralogy and Petrology* 137(2), 46-58.
- Simpson Jr, S. M. 1954. Least-squares polynomial fitting to gravitational data and density plotting by digital computers. *Geophysics* 19(2), 255-269.
- Spector, A., Grant, F. S. 1970. Statistical models for interpreting aeromagnetic data. *Geophysics* 35(2), 293-302.
- Stampfli, G. M. 2000. Tethyan oceans. *Geological Society of London. Special Publications* 173(1), 23.
- Tekeli, O. 1981. Subduction complex of pre - Jurassic age, northern Anatolia, Turkey. *Geology* 9(2), 68-72.
- Tirel, C., Gueydan, F., Tiberi, C., Brun, J. P. 2004. Aegean crustal thickness is inferred from gravity inversion. Geodynamical implications. *Earth and Planetary Science Letters* 228(3-4), 267-280.
- Ustaömer, T., Robertson, A. H. 1999. Geochemical evidence used to test alternative plate tectonic models for pre-Upper Jurassic (Palaeotethyan) units in the central Pontides, N Turkey. *Geological Journal* 34(2), 25-53.
- Yılmaz, Y. 1993. New evidence and model on the evolution of the southeast Anatolian orogen. *Geological Society of America Bulletin* 105(2), 251-271.
- Yılmaz, Y., Yıldırım, M. 1996. Geology and evaluation of the nap region (the metamorphic massifs) of the Southeast Anatolian Orogenic Belt. *Turkish Journal of Earth Sciences* 5(3), 21-38.